INFORMS Journal on Computing
Vol. 18, No. 2, Spring 2006, pp. 186–196
ISSN 1091-9856 | EISSN 1526-5528 | 06 | 1802 | 0186

DOI 10.1287/ijoc.1050.0138

A Discrete Adjoint Variable Method for Printed-Circuit Board Computer-Aided Design

Shirook M. Ali, Natalia K. Nikolova, Mohamed H. Bakr
Department of Electrical and Computer Engineering, McMaster University, Hamilton, Ontario, L8S 4K1 Canada
{sali@ece.mcmaster.ca, talia@mcmaster.ca, mbakr@mail.ece.mcmaster.ca}

We propose an adjoint-variable method for design sensitivity analysis of printed circuits and antennas where allowable perturbations in the design parameters are of a discrete type. We extend previous work on the sensitivity analysis of waveguide structures, where changes in the design parameters are stepwise, on-grid volumetric perturbations. Here, we explore the feasibility of such an approach in the case of printed-circuit board problems (with open boundaries) where perturbations relate to the shapes elements of infinitesimal thickness. We propose a complex-variable formulation of our approximate sensitivity analysis that improves its computational efficiency. The proposed technique offers significant increases in efficiency, accuracy, and convergence when compared to traditional sensitivity-analysis techniques. Its implementation is straightforward. The response and its gradient with respect to all possible design parameters are computed with at most two full-wave analyses—of the original and the adjoint problems. It operates on a fixed discretization grid where perturbations of grid nodes are not needed. We illustrate our technique through the sensitivity analysis of a microstrip line and a probe-fed printed patch antenna as well as the optimization of a printed Yagi antenna array.

Key words: sensitivity; adjoint variable method; printed antennas; computer-aided design (CAD)
History: Accepted by John W. Chinneck, Guest Editor for Special Issue on Operations Research in Electrical and Computer Engineering; received November 2003; revised July 2004; accepted February 2005.

1. Introduction

In the design of microstrip antennas and printed circuits, a designer can use simple and fast analysis approaches (models) such as transmission line and cavity models (Sainati 1996), empirical formulas (Pozar 1993), and microstrip-element libraries (Agilent Technologies 2000). However, these approaches suffer from a number of limitations due to the approximations that they introduce. These limitations are overcome in the numerical full-wave electromagnetic (EM) solvers (EM simulators). EM solvers are close numerical approximations of the basic EM laws, e.g., the system of Maxwell's equations, complemented by the respective boundary conditions and constitutive relations. These solvers are versatile with respect to complex boundary shapes and materials. The simulations typically feature good accuracy and completeness of the solution. These advantages are, however, at the expense of computational cost.

Currently, there is a great variety of numerical algorithms for full-wave EM analysis. For the purpose of sensitivity analysis, we classify the solvers according to their discretization grid (see Figure 1) as: (i) unstructured grid solvers (Figure 1a) and (ii) structured grid solvers (Figure 1b). Some of the popular solvers that are based on unstructured grids are the method of moments (MoM) (Harrington 1968), the finite-element method (FEM) (Jing 2002), the finite-difference time-domain discrete surface integral method (FDTD-DSI) (Madsen 1995), etc. Examples in the category of structured grid solvers include the time-domain transmission line method (TD-TLM) (Christopoulos 1995), the frequency-domain transmission line method (FD-TLM) (Johns and Chritopoulos 1994), the FDTD method based on Yee's (1966) cell, etc. A major difficulty with structured-grid solvers in sensitivity analysis is that perturbations in the shape parameters can take only certain snapped-to-grid values from a discrete set conforming to the grid. In contrast, with unstructured-grid solvers, the design parameters can take an infinite number of values within the acceptable design range.

The adjoint-variable method is an efficient technique for response sensitivity analysis, whose purpose is to obtain derivatives (sensitivities) of the response generated from the EM solver with respect to all design parameters. The latter are typically related to the shape and materials of the simulated structure. The method provides the sensitivity information through the solution of the original problem and what is called the *adjoint problem*. Thus, the response and its derivatives are obtained through two system analyses regardless of the number of design parameters.

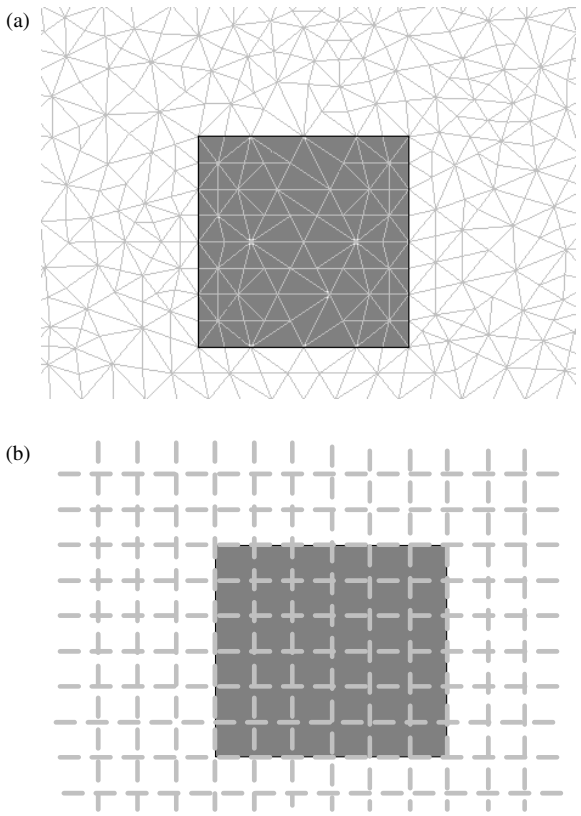

Figure 1 Discretization Grids in and Around an Object (Dark Cells) with a Numerical Solver

Notes. (a) Unstructured-grid discretization with triangular finite elements and (b) structured-grid discretization with rectangular elements.

Traditionally, the adjoint-variable method for design sensitivity analysis assumes the existence of the analytical derivatives of the system matrix with respect to the shape/material perturbations. With such derivatives, the response sensitivity computations are exact. While such derivatives may be possible (although rather difficult) to obtain with unstructured-grid solvers, they are simply not available when the solver uses a structured grid. These difficulties have prevented the use of adjoint-based sensitivity analysis with full-wave EM solvers. There is need in full-wave sensitivity analysis for approaches, which are simple to implement and do not require modification of the existing numerical codes.

There have been few successful applications of the traditional "exact" adjoint-variable method with high-frequency full-wave EM solvers. Exact sensitivities were considered with the FEM by Akel and Webb (2000), Lee et al. (1995), and Webb (2001, 2002), where analytical derivatives of the FEM system matrix with respect to the Cartesian coordinates of the mesh vertices are obtained. An analogous technique was used with the finite-element time domain (FETD) and the FDTD-DSI method by Chung et al. (2000, 2001), respectively.

Recently, approximate sensitivities were considered by Georgieva et al. (2002) for frequency-domain solvers on unstructured grids and applications with the MoM. There, the structure is rediscretized at each design iteration for every design parameter to accommodate, at most, 1% to 2% parameter perturbations. Analytical system matrix derivatives are not needed since they are approximated via finite differences.

In previous work, we (Ali et al. 2004) proposed a discrete finite-difference approach to adjoint-based sensitivity analysis for waveguide structures simulated with fixed-grid solvers. Here, we extend our approach to printed circuits and open radiation problems. The perturbations in the design parameters include infinitesimally thin metallic plates. They are realized by the metallization/demetalization of a single face of the perturbation-related grid cells. Our approach, whose complex-variable formulation is developed here, uses system matrix differences instead of their derivatives. A key feature of our approach is that the difference-system matrix need not be differentially small compared to the matrix itself in order to ensure accurate sensitivity results. These difference matrices are obtained by subtracting two predefined system matrices, which correspond to the original and perturbed systems. Because of its adjoint-variable nature, the proposed approach offers significant computational gain over the traditional finite-difference approximations that are applied directly at the level of the response.

Our approach is also advantageous when compared with the traditional "exact" adjoint-variable method. First, it does not require analytical derivatives of the system matrix. Thus, cumbersome (and often case-specific) analytical preprocessing is avoided. Second, there is no need for the computation of K system matrix derivatives, which is the major overhead with exact sensitivity analysis. Third, the technique is versatile—it accommodates all possible shape and material changes, as long as they conform to the discretization grid. Last but not least, the implementation of the proposed technique in existing numerical codes is straightforward.

We start with a brief description of the FD-TLM and its implementation with antenna problems in §2. A discussion of sensitivity analysis and its limitations with structured-grid solvers is given in §3. The proposed discrete adjoint-variable method for printed structures is described in §4. We illustrate the proposed technique through numerical examples in §5. Finally, conclusions are made in §6.

2. The FD-TLM for Printed Circuits and Antennas

We illustrate our proposed technique with applications using the FD-TLM, which is a full-wave

frequency-domain solver based on fixed structured grids. With this solver, time-harmonic field dependence is assumed and hence only space discretization is required. The computational space is discretized into rectangular cells (nodes) based on the symmetrical condensed node proposed by Johns and Christopoulos (1994). Each node in the 3-D space has 12 transmission lines (links) that couple to the corresponding links of the neighboring nodes. The scattering process is similar to that in the time-domain TLM (Christopoulos 1995). An equation is written for each link at each node in relation with the corresponding incident voltages from the neighboring nodes and the reflected voltages from the node itself. These voltages are delayed through propagation factors of the type

$$e^{-\gamma_l \Delta_c} \tag{1}$$

where γ_l is the propagation constant of the lth link and Δ_c is the corresponding cell size. The propagation factor in (1) is a function of the frequency, the local material properties, and the cell size. For the particular case of a lossless medium modeled by a uniform mesh of size Δ, $\gamma_l = j\beta_l$ where the phase constants β_l is

$$\beta_l = \frac{\omega\sqrt{\varepsilon\mu}}{2} \tag{2}$$

(Johns and Christopoulos 1994). Here, $\omega = 2\pi f_0$ where f_0 is the operating frequency; $\varepsilon = \varepsilon_r\varepsilon_0$ and $\mu = \mu_r\mu_0$ are the medium's permittivity and permeability for the respective link. The factor of 1/2 reflects the fact that the length of the link is half of the cell size.

When the equations for all the links in all the cells are put together, a complex linear system of equations is obtained:

$$\mathbf{A}(\mathbf{x}) \cdot \mathbf{v} = \mathbf{V}_s. \tag{3}$$

In (3), $\mathbf{A}$ is a $12N \times 12N$ (N is the total number of cells) complex coefficient matrix, $\mathbf{v}$ is the vector of incident voltages (the complex solution vector), and $\mathbf{V}_s$ is the source vector. The matrix $\mathbf{A}$ is related to the parameters of the medium and the boundary conditions of the problem. Thus, it is a function of the vector of design parameters $\mathbf{x}$, $\mathbf{x} = [x_1 \cdots x_K]^T$, where K is the total number of design parameters. Responses used to measure the performance of the system—such as the transmission/reflection coefficients, input impedance, etc.—are computed by post-processing the solution $\mathbf{v}$.

Full-wave analysis of printed structures using the FD-TLM is possible. The substrate is modeled by TLM cells with constitutive parameters ε_d and μ_d, which are incorporated in the propagation factor γ_l of the medium (1). Similarly, in the air, $\varepsilon = \varepsilon_0$ and $\mu = \mu_0$. The printed metallizations are modeled as infinitesimally thin metallic plates. They have zero thickness and they are located between the nodes, i.e., the incident voltages on the links in the normal y-direction

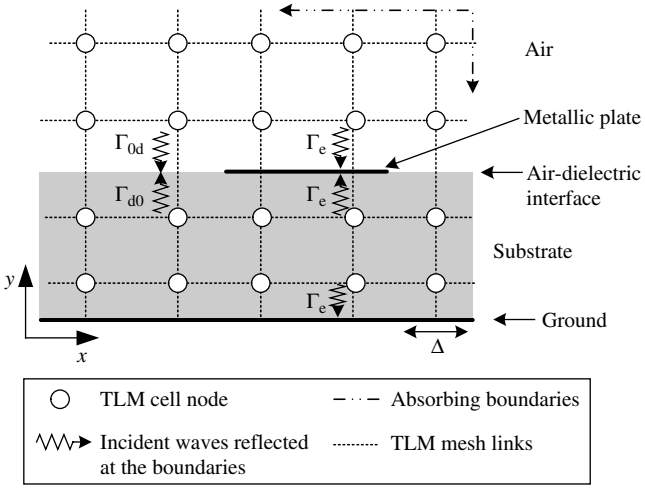

Figure 2 Discretization Mesh of a Possible Printed Structure Modeled with the TLM Nodes

(see Figure 2) are reflected back to the center of the same cell with a reflection coefficient $\Gamma_e = -1$. This applies to the links of the cells above (in the air) and below (in the dielectric) the metallic plate. The cells in the air at the air-dielectric interface have a reflection coefficient $\Gamma_{0d} = (Z_d - Z_0)/(Z_d + Z_0)$, where $Z_d = \sqrt{\mu_d/\varepsilon_d}$ is the intrinsic impedance of the substrate, and $Z_0 = \sqrt{\mu_0/\varepsilon_0}$ is that of air. Likewise, the incident voltages in the cells within the substrate at the air-dielectric interface are reflected back with a reflection coefficient $\Gamma_{d0} = (Z_0 - Z_d)/(Z_d + Z_0)$.

The absorbing boundary conditions used to terminate the computational domain are the zero reflection termination (ZRT) boundaries proposed by Pasalic et al. (1999). They simulate reflection-free wave propagation and terminate our computational domain from all sides except from the bottom side, where a ground plane is placed. The ground plane is modeled as a perfect conductor with $\Gamma_e = -1$. Figure 2 illustrates the FD-TLM computational domain for a printed structure.

3. Sensitivity Analysis and Numerical EM Solvers

The purpose of sensitivity analysis is to measure the rate of change of a response function f with respect to changes in a set of design parameters $\mathbf{x}$. Mathematically, the sensitivity is given by the gradient of f with respect to $\mathbf{x}$, i.e., $\nabla_x f$. This information is important in a number of engineering applications such as gradient-based optimization, yield, and tolerance analysis.

Assume that f is a general scalar function that represents a response of interest for the linear system in (3). This function may have an explicit dependence on $\mathbf{x}$, and an implicit dependence through the state

variable $\mathbf{v}$, i.e., $f(\mathbf{x}, \mathbf{v}(\mathbf{x}))$. Our objective is to determine the sensitivity of the response f with respect to $\mathbf{x}$, i.e.,

$$\nabla_{\mathbf{x}} f, \quad \text{subject to} \quad \mathbf{A} \cdot \mathbf{v} = \mathbf{V}_s \tag{4}$$

where $\nabla_{\mathbf{x}}$ is defined as a row operator

$$\nabla_{\mathbf{x}} = \left[\frac{\partial}{\partial x_1} \cdots \frac{\partial}{\partial x_K} \right]. \tag{5}$$

A simple technique toward the solution of (4) uses finite differences applied directly to the response. The first-order forward or backward approximations require $K+1$ full-wave simulations. A second-order accurate estimation can be obtained using central finite differences, which requires $2K+1$ system analyses.

A more accurate and efficient technique is the adjoint-variable method, which in contrast to response-level finite differences, requires at most two full-wave simulations to evaluate (4) regardless of K. In the next sections, we present a brief background of the original "exact" adjoint-variable method and illustrate the limitations involved in its implementation with EM solvers based on structured grids such as the FD-TLM.

3.1. Exact Sensitivities for Linear Problems: Background

The complex system (3) can be represented as a real system of the form

$$\mathbf{A}^R \cdot \mathbf{v}^R = \mathbf{V}_s^R \tag{6}$$

where

$$\mathbf{A}^R = \begin{bmatrix} \Re\mathbf{A} & \Im\mathbf{A} \\ -\Im\mathbf{A} & \Re\mathbf{A} \end{bmatrix}, \quad \mathbf{v}^R = \begin{bmatrix} \Re\mathbf{v} \\ \Im\mathbf{v} \end{bmatrix}, \quad \text{and} \quad \mathbf{V}_s^R = \begin{bmatrix} \Re\mathbf{V}_s \\ \Im\mathbf{V}_s \end{bmatrix}. \tag{7}$$

In (7), $\Re$ and $\Im$ denote the real and imaginary parts of the corresponding matrix or vector. Notice that the size of the real system (6) is twice that of the complex system (3).

The exact adjoint-variable sensitivity expression with respect to, for example, the kth design parameter x_k, is

$$\frac{df}{dx_k} = \frac{\partial f}{\partial x_k} + (\boldsymbol{\lambda}^R)^T \left[\frac{\partial \mathbf{V}_s^R}{\partial x_k} - \frac{\partial \mathbf{A}^R}{\partial x_k} \bar{\mathbf{v}}^R \right], \quad k = 1, \ldots, K \tag{8}$$

(Haug et al. 1986). The partial derivative $\partial f / \partial x_k$ represents the explicit dependence of f on x_k; $\bar{\mathbf{v}}^R$ is a constant vector representing the solution of (3) at the current design; $\partial \mathbf{A}^R / \partial x_k$ is the derivative of the system matrix with respect to x_k; $\partial \mathbf{V}_s^R / \partial x_k$ is the derivative of the excitation with respect to x_k; and $\boldsymbol{\lambda}^R$ is the adjoint vector $(\boldsymbol{\lambda}^R)^T = [(\Re\boldsymbol{\lambda})^T \ (\Im\boldsymbol{\lambda})^T]$. It is the solution of the adjoint problem defined as

$$\begin{bmatrix} \Re\mathbf{A} & \Im\mathbf{A} \\ -\Im\mathbf{A} & \Re\mathbf{A} \end{bmatrix}^T \begin{bmatrix} \Re\boldsymbol{\lambda} \\ \Im\boldsymbol{\lambda} \end{bmatrix} = [\nabla_{\Re\mathbf{v}} f \quad \nabla_{\Im\mathbf{v}} f]^T. \tag{9}$$

The right-hand term in (9) is referred to as the *adjoint excitation*, which contains the derivatives of the objective function with respect to the state variables. Once the solution $\mathbf{v}^R$ in the original problem is obtained, the sensitivity information with respect to all K design parameters can be found after solving (9) for the adjoint solution $\boldsymbol{\lambda}^R$. In our implementation, we assume that the original problem (6) has been solved.

3.2. Sensitivity-Analysis Limitations with Structured-Grid Solvers

The major difficulty with the sensitivity expression (8) in the case of structured grids is in finding the derivatives of the system matrix with respect to changes in the design parameters, i.e., $\partial\mathbf{A}/\partial x_k$, $k = 1, \ldots, K$.

Consider the case where the design parameter x_k represents the length of the metallic printed patch shown in Figure 3a, i.e., $x_k = L$. Assume that we want to accommodate a perturbation of $\Delta x_k = \Delta L$ in the length L. One way to perturb is to stretch all the patch cells uniformly by $\Delta x_k / n$ (where n is the original number of cells in x_k) in the z-direction. This, however, also changes the location of the excitation (the probe) from its original location at (x_0, z_0) to a new perturbed location at $(x_0, z_0 + \Delta L/n)$. The resulting problem is different from the original one since the location of the excitation point is now different (see Figure 3b). This is not acceptable since the source location may be a separate design parameter.

An alternative way to perturb is to assume local discrete perturbations in x_k, i.e., we assume that perturbations in x_k take integer multiples of the cell size, for example $\Delta x_k = \Delta_c$, in the respective direction. This means that if $x_k = n\Delta_c = L$ is the original design-parameter value, then the perturbed length is $x_k^p = (n+1)\Delta_c = L + \Delta_c$ (see Figure 3c). Thus, we keep the mesh and the cell size unchanged, and we add a whole cell to the end of the patch to accommodate the perturbation. The effect of such a discrete perturbation on the computation of the difference-system matrices in the sensitivity formula is discussed in subsequent sections.

To accommodate the assumed discrete type of perturbations, a new sensitivity expression is needed that can include coarse stepwise changes in the system-matrix coefficients. In the next section, we derive a general sensitivity formula for perturbations of the discrete type. We limit the discussion to linear systems. The technique is not limited to the FD-TLM.

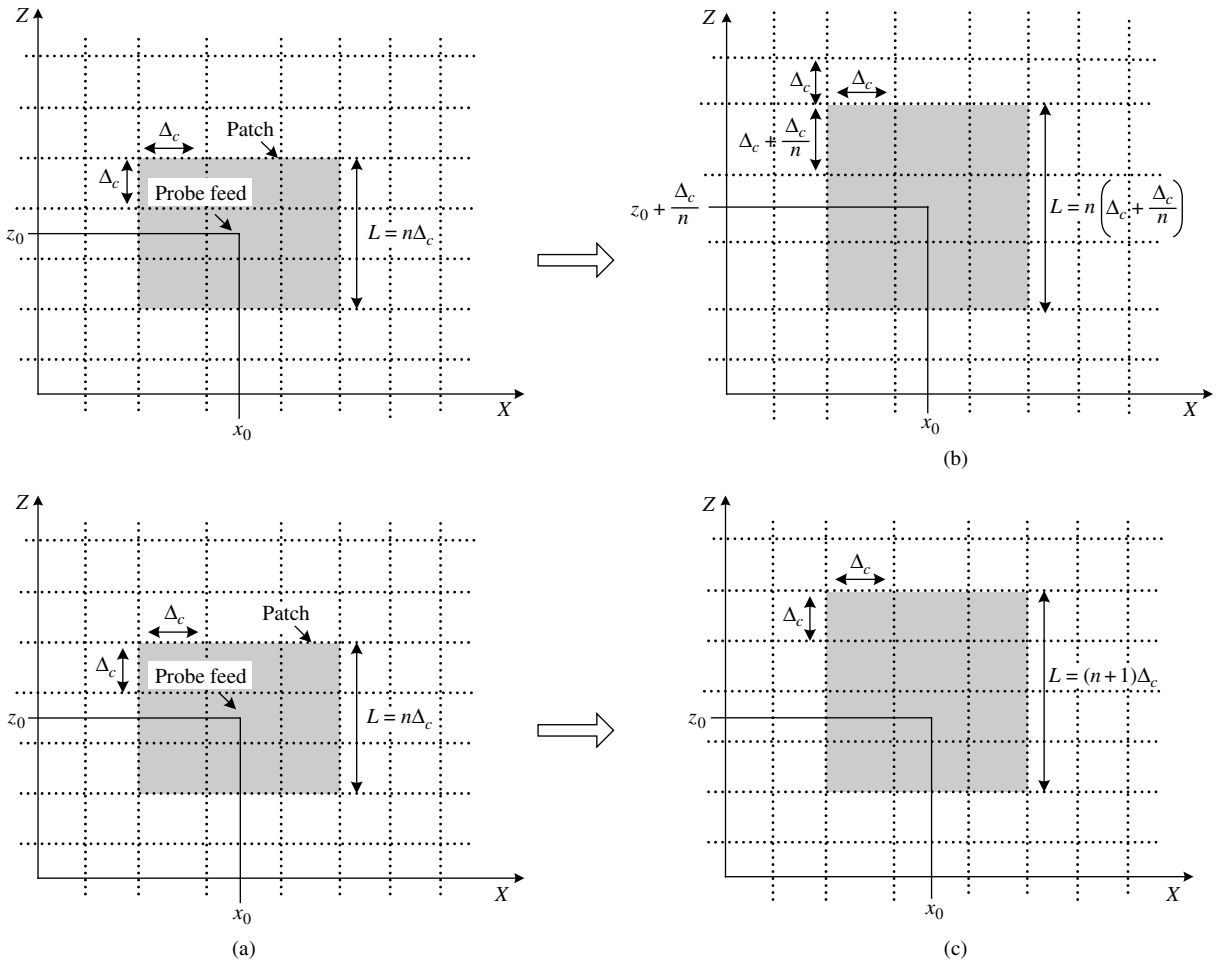

Figure 3 **Illustration of a Perturbation ΔL in the Length of the Patch L (Top View) by Stretching the Cells in the Respective Direction vs. a Discrete On-Grid Perturbation**

Notes. (a) The original problem; (b) the stretched-cell perturbed problem; and (c) the discrete perturbed problem.

4. Approximate Sensitivities for Printed-Antenna Problems

4.1. Real-System Representation

We restrict the perturbations in the design parameters to the smallest on-grid perturbation of Δx_k. Accordingly, the perturbed system matrix is $\mathbf{A}(\mathbf{x} + \Delta x_k \cdot \mathbf{e}_k)$, where $\mathbf{e}_k = [0, \ldots, \underset{k\text{th}}{1}, 0, \ldots]^T$. The resultant complex perturbed system of equations corresponding to (3) becomes

$$\mathbf{A}_k \cdot \bar{\mathbf{v}}_k = \mathbf{V}_{k,s}, \quad k = 1, \ldots, K \tag{10}$$

where $\mathbf{A}_k = \mathbf{A}(\mathbf{x} + \Delta x_k \cdot \mathbf{e}_k)$, $\mathbf{V}_{k,s} = \mathbf{V}_s(\mathbf{x} + \Delta x_k \cdot \mathbf{e}_k)$ is the excitation after the perturbation Δx_k takes place, and $\bar{\mathbf{v}}_k$ is the respective solution:

$$\bar{\mathbf{v}}_k = \bar{\mathbf{v}} + \Delta \mathbf{v}_k, \quad k = 1, \ldots, K. \tag{11}$$

Usually, the excitation is insensitive to changes in the geometry and materials, in which case $\mathbf{V}_{k,s}$ is simply equal to $\mathbf{V}_s$ in the original unperturbed problem. In (11), $\bar{\mathbf{v}}$ is the solution of the original unperturbed problem (3), and $\Delta \mathbf{v}_k$ is the change in the solution due to Δx_k. In this real form, the kth perturbed system solution $\bar{\mathbf{v}}_k^R$ satisfies

$$\mathbf{A}_k^R \cdot \bar{\mathbf{v}}_k^R = \mathbf{V}_{k,s}^R, \quad k = 1, \ldots, K \tag{12}$$

where

$$\mathbf{A}_k^R = \begin{bmatrix} \Re\mathbf{A}_k & \Im\mathbf{A}_k \\ -\Im\mathbf{A}_k & \Re\mathbf{A}_k \end{bmatrix}, \quad \bar{\mathbf{v}}_k^R = \begin{bmatrix} \Re\bar{\mathbf{v}}_k \\ \Im\bar{\mathbf{v}}_k \end{bmatrix}, \quad \text{and} \quad \mathbf{V}_{s,k}^R = \begin{bmatrix} \Re\mathbf{V}_{s,k} \\ \Im\mathbf{V}_{s,k} \end{bmatrix}, \quad k = 1, \ldots, K. \tag{13}$$

The approximate adjoint sensitivity in the case of a real-valued objective function f and the system (12) is given by Ali et al. (2004) and Bakr and Nikolova (2003) as

$$\frac{df}{dx_k} \simeq \frac{\partial f}{\partial x_k} + (\boldsymbol{\lambda}^R)^T \left[\frac{\Delta_k \mathbf{V}_s^R}{\Delta x_k} - \frac{\Delta_k \mathbf{A}^R}{\Delta x_k} \cdot \bar{\mathbf{v}}_k^R \right], \quad k = 1, \ldots, K. \tag{14}$$

As in (8), $\partial f/\partial x_k$ represents the explicit dependence of f on changes in x_k, and $\boldsymbol{\lambda}^R$ is the real-valued adjoint variable vector, which is the solution of (9). The remaining terms in (14) are the difference-system matrix with respect to x_k, $\Delta_k \mathbf{A}^R = \mathbf{A}_k^R - \mathbf{A}^R$, and the difference in the excitation vector due to changes in x_k, $\Delta_k \mathbf{V}_s^R = \mathbf{V}_{k,s}^R - \mathbf{V}_s^R$.

The sensitivity expression (14) is approximate because the difference-matrix ratio $\Delta_k \mathbf{A}^R/\Delta x_k$ need not be an actual representation of the analytical derivative $\partial \mathbf{A}^R/\partial x_k$. Whereas the exact formula (8) fails due to inadequate approximation of $\partial \mathbf{A}^R/\partial x_k$, (14) gives excellent accuracy. The advantage comes from the fact that in (14), $\bar{\mathbf{v}}_k^R$ is the exact solution of the "perturbed" original problem (12). In contrast, (8) uses $\bar{\mathbf{v}}^R$, which is an exact solution to the "unperturbed" system (6).

4.2. Complex-System Representation

In most EM problems, it is required to find the sensitivity of a complex response f subject to a complex linear system of equations. Then, two separate sensitivity expressions in the form of (14), for $\Re f$ and $\Im f$, are used in conjunction with two separate adjoint problems in the form of (9). Here, we derive a more general complex-valued approximate sensitivity expression and show that as long as the complex response function is an analytic function of the complex state variable $\mathbf{v}$, only one adjoint problem needs to be solved.

The complex response f can be expressed as

$$f = \Re f + j\Im f \tag{15}$$

where $j = \sqrt{-1}$. We apply an approach used to derive the exact sensitivity formula for complex systems and complex responses (Nikolova et al. 2004) to our approximate real-valued expression (14). Using the Cauchy-Riemann equations,

$$\begin{aligned} \nabla_{\Re \mathbf{v}} \Re f &= \nabla_{\Im \mathbf{v}} \Im f = \Re \nabla_{\mathbf{v}} f \\ -\nabla_{\Im \mathbf{v}} \Re f &= \nabla_{\Re \mathbf{v}} \Im f = \Im \nabla_{\mathbf{v}} f \end{aligned} \tag{16}$$

we can show that the adjoint solution corresponding to the sensitivity of $\Im f$, $\boldsymbol{\lambda}(\Im f)$, relates to the adjoint solution corresponding to the sensitivity of $\Re f$ as

$$\boldsymbol{\lambda}(\Im f) = j\boldsymbol{\lambda}(\Re f) \tag{17}$$

where $\boldsymbol{\lambda}$ is the complex adjoint-variable vector $\boldsymbol{\lambda} = \Re\boldsymbol{\lambda} + j\Im\boldsymbol{\lambda}$; see (9). It is the solution to Nikolova et al. (2004)

$$\mathbf{A}^H \cdot \boldsymbol{\lambda} = [\nabla_{\mathbf{v}} f]^H \tag{18}$$

where H denotes the conjugate transpose of the respective matrix or vector, and $\nabla_{\mathbf{v}} f = \nabla_{\Re \mathbf{v}} f - j\nabla_{\Im \mathbf{v}} f$. Accordingly, our complex discrete sensitivity expression is

$$\frac{df}{dx_k} = \frac{\partial f}{\partial x_k} + \boldsymbol{\lambda}^H \cdot \left[\frac{\Delta_k \mathbf{V}_s}{\Delta \mathbf{x}_k} - \frac{\Delta_k \mathbf{A}}{\Delta \mathbf{x}_k} \bar{\mathbf{v}}_k \right], \quad k = 1, \ldots, K. \tag{19}$$

In (19), $\Delta_k \mathbf{V}_s$ is the difference-complex-excitation vector due to Δx_k, and $\Delta_k \mathbf{A}$ is the difference complex coefficient matrix in x_k due to Δx_k.

The difference excitation vector $\Delta_k \mathbf{V}_s$ can be easily found using finite differences if the analytical derivative $\partial \mathbf{V}_s/\partial x_k$ is not available. The difference matrix $\Delta_k \mathbf{A}$ is mostly zeros except for those coefficients that correspond to the set of links at changed boundaries due to Δx_k. As an example, if a node is at the air-dielectric interface with $\Gamma = \Gamma_{0d}$ or Γ_{d0}, then an infinitesimally thin metallization of one face of the cell changes Γ to $\Gamma = \Gamma_e = -1$. In the case of demetallization of a cell face, the respective reflection coefficient will change from $\Gamma = \Gamma_e = -1$ to $\Gamma = \Gamma_{0d}$ or Γ_{d0}. The advantages of such a "discrete" type of perturbations are: (i) the perturbations in the design parameters are local, and hence they do not affect other geometrical details; (ii) the initial mesh is preserved during the sensitivity analysis and hence, no remeshing is needed during optimization; and (iii) there is no need for the computation of the perturbed system matrix for every perturbation since the affected coefficients in the system matrix are predefined. Thus, computation of $\Delta_k \mathbf{A}$ is done as the difference between two predefined matrices—of the unperturbed and perturbed in x_k structures.

The elements of $\Delta \mathbf{v}_k$, on the other hand, are not known. However, since $\Delta_k \mathbf{A}$ is mostly zero, we need to find only those elements of $\Delta \mathbf{v}_k$ that correspond to the set of links, for example L_i, which are related to the nonzero $\Delta_k \mathbf{A}$-coefficients. Based on the perturbation theory (Harrington 1961), an approximation of these $\Delta \mathbf{v}_k$ elements is developed through a mapping of the field between the original and perturbed problems (Ali et al. 2004, Bakr and Nikolova 2003). The numerical implementation of this concept is discussed in more detail in the next section.

The proposed technique can be summarized in the following steps:

1. *Parameterization*: Specify the set of links L_i whose corresponding $\mathbf{A}$-coefficients are affected by the perturbations Δx_k, $k = 1, \ldots, K$.
2. *Original system analysis*: (a) Solve the original system (3); (b) store the incident voltages for all the links in the set L_i; (c) store the incident voltages in the observation domain to be used in the computation of the adjoint excitation (18).
3. *Adjoint analysis*: Solve the adjoint problem (18) and store $\boldsymbol{\lambda}$ in the locations that correspond to the set L_i and the nonzero elements of $\Delta_k \mathbf{V}_s$.

4. *Field mapping*: Perform the mapping between the solutions of the original problem and the perturbed problem for the elements of $\tilde{\mathbf{v}}$ that correspond to L_i.

5. *Sensitivities estimation*: Evaluate the sensitivities using (19) for all K parameters.

5. Numerical Implementation and Examples

We illustrate implementation of the proposed discrete technique through the sensitivity computations of a microstrip line and a probe-fed printed patch antenna. We also show the integration of our technique with gradient-based optimization through the optimization of an electromagnetically coupled microstrip Yagi antenna array. The optimizer uses responses and their sensitivities, which are computed with our discrete-sensitivity analysis algorithm.

5.1. Characteristic Impedance of a Microstrip Line

The proposed technique is first tested with an example where the sensitivity of the characteristic impedance Z_c of the microstrip line shown in Figure 4 is computed at 3 GHz. The excitation voltage is depicted by the vertical arrows beneath the strip. The permittivity of the substrate is $\varepsilon_r = 2.32$. Its height is $h = 2$ mm. The symmetry of the structure is used and, thus, only half of it is simulated. The design parameter is the width of the line, i.e., $\mathbf{x}_k = [W]$, $k = 1$. The derivative dZ_c/dW is computed in two different ways: as a central finite difference (CFD) approximation and with our adjoint technique. The sensitivity of Z_c is evaluated in the range from $W = 4\Delta$ to $W = 10\Delta$, where $\Delta = 1$ mm is the TLM grid size. In the CFD estimation, for each $W^{(i)}$, the simulator is invoked twice to perform the forward and backward analyses for $W^{(i)} \pm \Delta W^{(i)}$, where $\Delta W^{(i)} = \Delta$. Thus, the $\partial Z_c/\partial W$ derivatives are computed as

$$\frac{\partial Z_c}{\partial W} \simeq \frac{Z_c(W^{(i)} + \Delta W^{(i)}) - Z_c(W^{(i)} - \Delta W^{(i)})}{2\Delta}. \tag{20}$$

In our discrete adjoint sensitivity estimation, the sensitivity of Z_c is evaluated using (19). The derivative of the excitation (see Figure 5) with respect to the width of the microstrip line is computed with finite differences:

$$\frac{\Delta \mathbf{V}_s}{\Delta W^{(i)}} \simeq \frac{\mathbf{V}_s(W^{(i)} + \Delta W^{(i)}) - \mathbf{V}_s(W^{(i)})}{\Delta}. \tag{21}$$

The difference-system matrix $\Delta_W \mathbf{A}$ is

$$\Delta_W \mathbf{A} = \mathbf{A}(W^{(i)} + \Delta W^{(i)}) - \mathbf{A}(W^{(i)}). \tag{22}$$

In (22), both the original matrix $\mathbf{A}(W^{(i)})$ and the perturbed matrix $\mathbf{A}(W^{(i)} + \Delta W^{(i)})$ are already known.

The perturbed solution vector $\bar{\mathbf{v}}_W$ is approximated using a one-to-one mapping between the perturbed and the original field solution based on perturbation theory (Harrington 1961). Thus, we avoid performing K system analyses as suggested by (10)–(11). An example is illustrated in Figure 6a. Consider the approximated incident voltages $\tilde{\mathbf{v}}_W \approx \bar{\mathbf{v}}_k$ in the perturbed problem for $W + \Delta W$. At $x = W/2 + \Delta x$, their values under and above the metal strip are taken equal to the corresponding incident voltages of the unperturbed problem at $x = W/2$:

$$\tilde{\mathbf{v}}_W(x = W/2 + \Delta x) = \bar{\mathbf{v}}(x = W/2). \tag{23}$$

In the case where the problem is simulated in full, i.e., no symmetry is used, the mapping should be done for both the left edge (at $x = -W/2$) and the

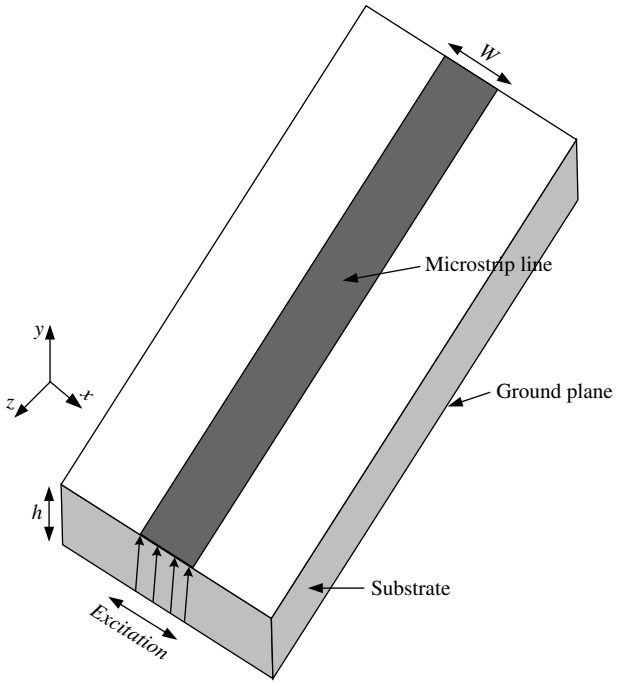

Figure 4 **Microstrip Line: The Vertical Arrows Depict the Incident Voltage Excitation**

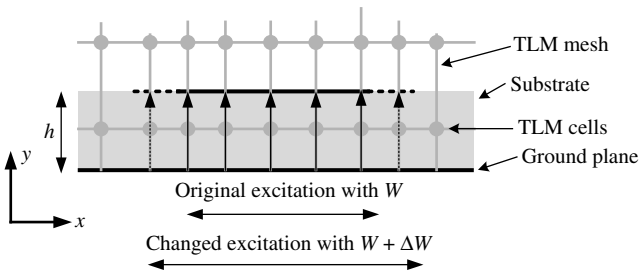

Figure 5 **Perturbation of the Strip Width and the Associated Change in the Excitation Vector $\mathbf{V}_s$**

Notes. Notice that the excitation voltage is now being added to the cells beneath the "metalized" faces (dashed line).

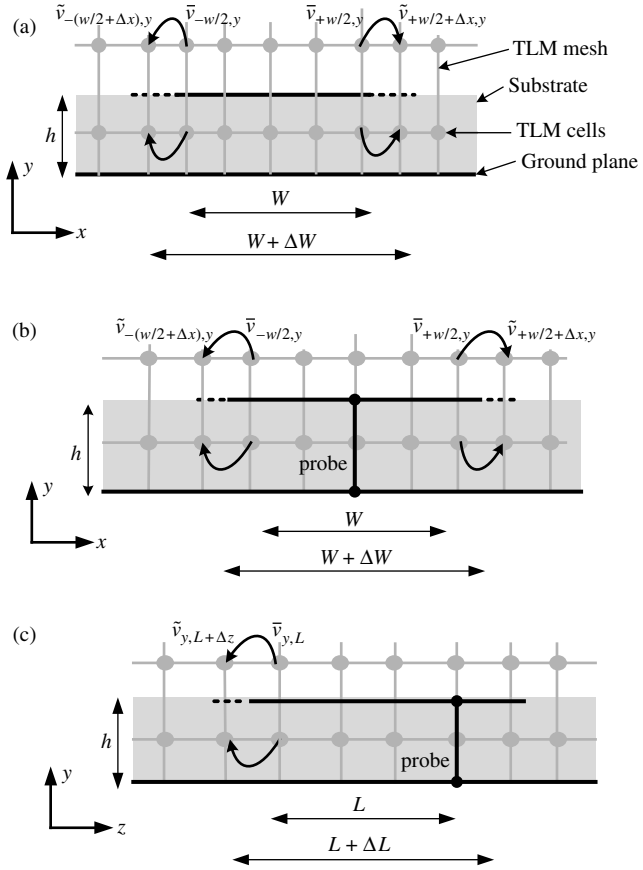

Figure 6 **Mapping of the Field: (a) for an Assumed Perturbation of the Microstrip Width, ΔW; (b) for an Assumed Perturbation in the Patch Antenna Width W; and (c) for an Assumed Perturbation in the Patch Antenna Length L**

right edge (at $x = +W/2$) of the strip line to preserve the symmetry of the structure with respect to the observation point.

The discrete sensitivities are computed and compared with the CFD derivatives as shown in Figure 7. Good agreement is achieved. This trend shows that the accuracy of the proposed adjoint technique is of the same order as the CFD. Our technique, however, is much more efficient.

For the case where the sensitivities are computed with the CFD approximation, the gradient computation requires two additional matrix fills and two system analyses per each $W^{(i)}$. In our discrete-sensitivity technique, only one additional system analysis of the adjoint problem is required. The five full-wave simulations required to compute the Z_c and $\nabla_W Z_c$ using CFD took 89.6 seconds compared to 31.2 seconds using our discrete approach. These were measured on a PC with a Pentium 4 3.0 GHz processor. The computational savings are more pronounced as the number of design parameters increases ($K > 1$). This is illustrated in our next examples.

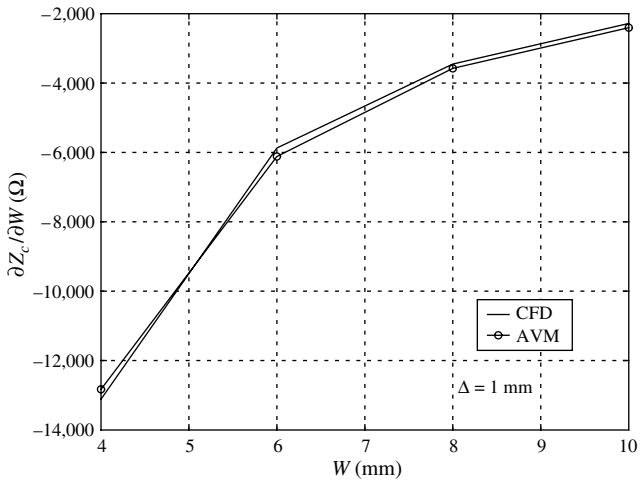

Figure 7 **Objective Sensitivities of the Microstrip Line Example with $\Delta = 1$ mm for Different Values of W**

5.2. Sensitivity of the Input Impedance for a Printed Patch Antenna

In this example, we test the proposed technique with the sensitivities of the real part of the input impedance R_{in} of a printed patch antenna shown in Figure 8 at 4.4 GHz. The patch is probe-fed at $W/2$ and $L/4$, where W and L are the physical width and length, respectively. The thickness of the substrate supporting the patch is $h = 1.524$ mm with permittivity $\varepsilon_r = 2.2$. The computational domain is discretized with a uniform TLM mesh of $\Delta = 1.524$ mm. The domain size is $N = 35 \times 8 \times 29$ nodes.

The sensitivity of R_{in} is computed with respect to the physical length and width of the patch, i.e., $\nabla_{\mathbf{x}} R_{in} = [\partial R_{in}/\partial L \;\; \partial R_{in}/\partial W]$, and $\mathbf{x} = [L \;\; W]^T$. These sensitivities are computed (i) as a finite-difference approximation, and (ii) using our discrete-adjoint technique.

The computation of $\tilde{\mathbf{v}}_k$, $k = 1, \ldots, K$, involves the mapping of the field in the x-direction to accommodate perturbations in W (see Figure 6b) and in the z-direction for the perturbations in L (see Figure 6c).

Figures 9 and 10 show a comparison between the sensitivities computed with finite-difference approximations—both CFD and forward finite differences (FFD)—and with our discrete sensitivity

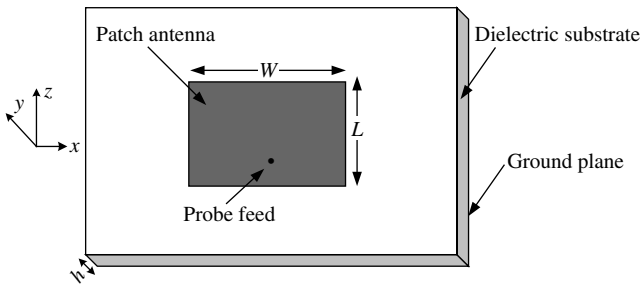

Figure 8 **Probe-Fed Patch Antenna**

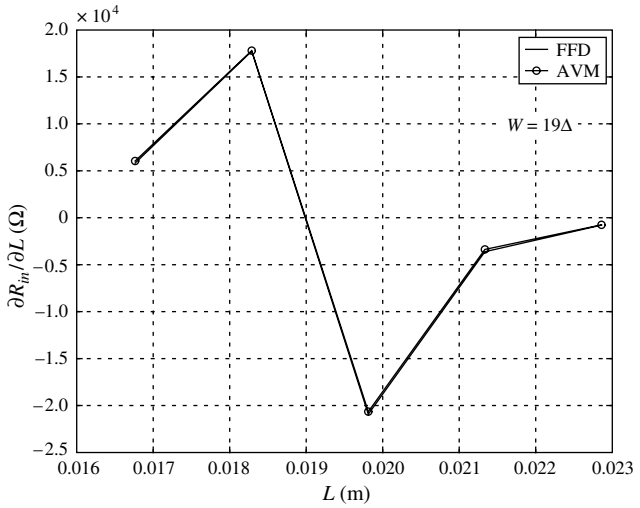

Figure 9 **Sensitivities of the Patch Antenna at $W = 19\Delta$ for Different Values of L**

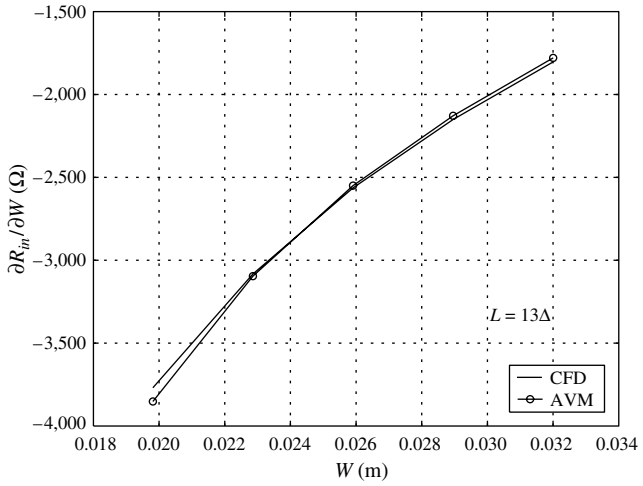

Figure 11 **Sensitivities of the Patch Antenna at $L = 13\Delta$ for Different Values of W**

estimation for a sweep of the parameter L. The sensitivities for a sweep in the parameter W are shown in Figures 11 and 12, respectively. A good match is obtained in both cases.

The simulation time required to compute R_{in} and $\nabla_{\mathbf{x}} R_{in}$ using a PC with a Pentium 4 3.0 GHz processor was 1,522.3 seconds with CFD, 913.4 seconds with the FFD, and 327.2 seconds with our discrete approach. Notice that the accuracy of our computed derivatives is comparable with that of the second-order CFD. Hence, we achieve computational savings over the CFD approximation of a factor of about 4.7 times for $K = 2$.

5.3. Optimization of an Electromagnetically Coupled Yagi Antenna Array

This example illustrates an application where sensitivity information is used in antenna design. We optimize the electromagnetically coupled Yagi antenna array shown in Figure 13 using gradient-based optimization. The optimization is carried out using a *minimax* optimizer (Madsen et al. 2002). It is integrated with our FD-TLM simulator and is supplied with the Jacobian matrix computed once with our discrete adjoint technique and a second time (in a separate optimization) with FFD at the level of the response.

The Yagi array consists of a driven element, a reflector, and two directors. The driven element is electromagnetically coupled to a feeding quarter-wavelength line that is in turn coupled to a feeding microstrip line. The array, its elements, and the ground plate are assumed to be made of perfect conductors. The used substrate has permittivity $\varepsilon_r = 10.2$.

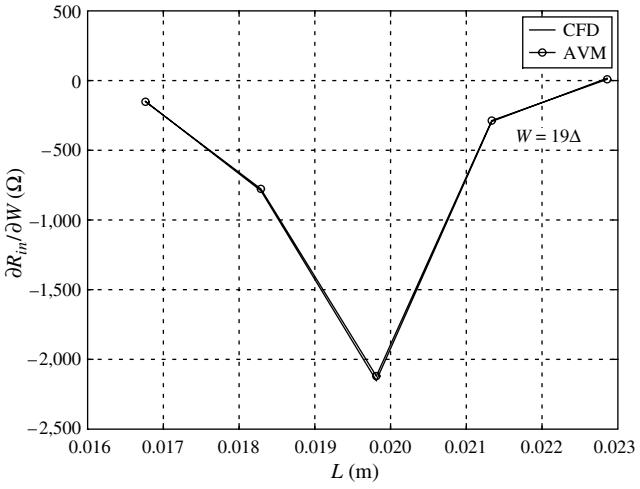

Figure 10 **Sensitivities of the Patch Antenna at $W = 19\Delta$ for Different Values of L**

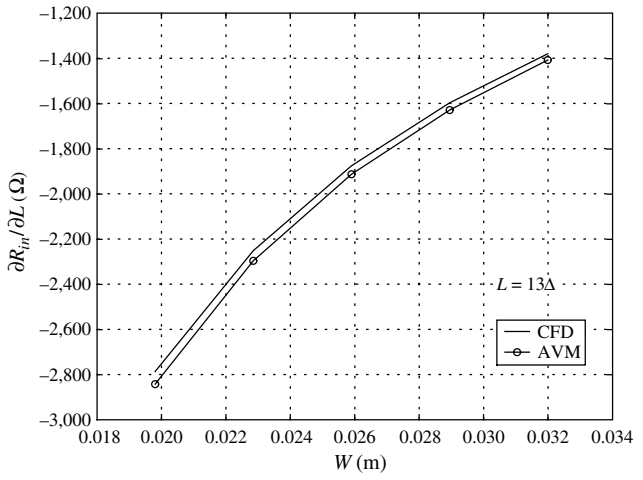

Figure 12 **Sensitivities of the Patch Antenna at $L = 13\Delta$ for Different Values of W**

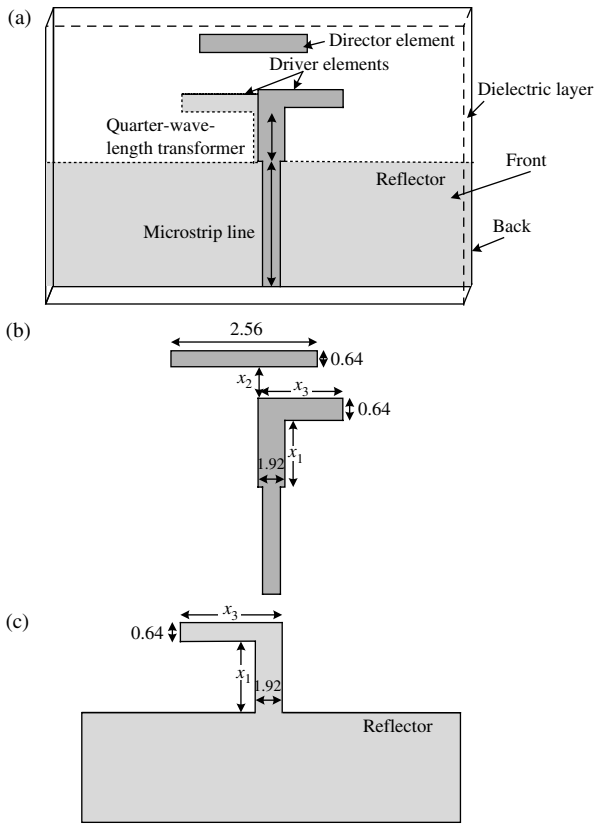

Figure 13 **Electromagnetically Coupled Yagi Antenna Array**

Notes. All units are in mm. (a) 3D geometry, (b) top layer, and (c) bottom layer.

Our design specification is

$$|S_{11}| < -10 \text{ dB} \quad \text{for } 9.7 \text{ GHz} < f_0 < 11.6 \text{ GHz} \qquad (24)$$

where $|S_{11}|$ is the return loss of the antenna, which we would like to minimize within the specified frequency range. The vector of design parameters is $\mathbf{x} = [x_1 \ x_2 \ x_3]^T$. It parameters have initial values $\mathbf{x}^o = [5.76 \ 1.28 \ 4.48]^T$ mm. The design specification is met in 14 iterations with optimal design parameters $\mathbf{x}^* = [7.68 \ 2.56 \ 3.2]^T$ mm. The cost of each design iteration is 23.4 min, using the derivatives computed from our discrete technique, and 35.1 min when the derivatives are computed using FFD at the level of the response. Hence, the complete design process using our technique required about 5.46 hours while that with FFD derivatives required 8.19 hours. The savings in computation time for the same design outcome is obvious. The initial and optimal responses are given in Figure 14.

6. Conclusions

We propose a novel numerical technique for sensitivity analysis intended for printed-circuit and antenna structures simulated with fixed structured-grid full-wave solvers. The geometrical changes are defined as stepwise perturbations. Two full-wave simulations are sufficient for computation of a response and its sensitivities regardless of the number and nature of the design parameters. The technique offers saving by, at least, a factor equal to the number of design parameters, which in turn reduces the time required by gradient-based optimization, statistical, and yield analyses. Analytical derivatives of the system matrix are not needed. The proposed technique features simplicity and good accuracy. Its implementation with existing frequency-domain simulators is straightforward. Our approach is illustrated through sensitivity analysis and optimization of a number of printed structures.

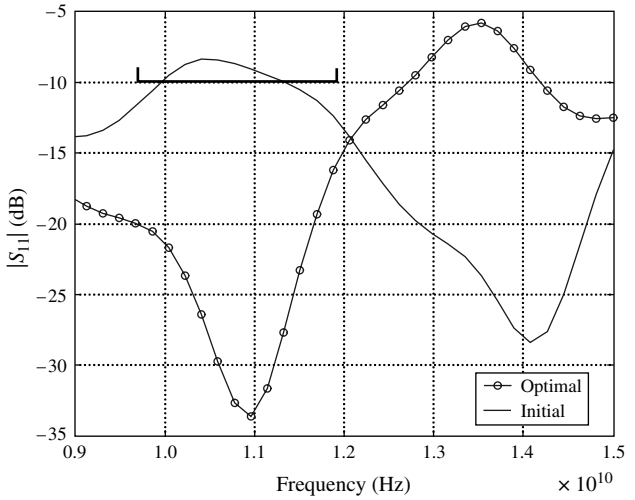

Figure 14 **The Initial and Optimal Responses ($|S_{11}|$) vs. Frequency for the Electromagnetically Coupled Yagi Antenna Array**

References

Agilent Technologies. 2000. Agilent Momentum, Version 4.0. Santa Rosa, CA.

Akel, H., J. P. Webb. 2000. Design sensitivities for scattering-matrix calculation with tetrahedral edge elements. *IEEE Trans. Magnetics* **36** 1043–1046.

Ali, S. M., N. K. Nikolova, M. H. Bakr. 2004. Sensitivity analysis with full-wave EM solvers based on structured grids. *IEEE Trans. Magnetics* **40** 1521–1529.

Bakr, M. H., N. K. Nikolova. 2003. An adjoint variable method for frequency domain TLM problems with conducting boundaries. *IEEE Microwave Wireless Components Lett.* **13** 408–410.

Christopoulos, C. 1995. *The Transmission-Line Modeling Method TLM*. IEEE Press, New York.

Chung, Y., C. Cheon, S. Hahn. 2000. Optimal shape design of microwave device using FDTD and design sensitivity analysis. *IEEE Trans. Microwave Theory Tech.* **48** 2289–2296.

Chung, Y. S., C. C. Cheon, I. H. Park, S. Y. Hahn. 2001. Optimal design method for microwave device using time domain method and design sensitivity analysis—Part I: FETD case. *IEEE Trans. Magnetics* **37** 3289–3293.

Georgieva, N. K., S. G. Glavic, M. H. Bakr, J. W. Bandler. 2002. Feasible adjoint sensitivity technique for EM design optimization. *IEEE Trans. Microwave Theory Tech.* **50** 2751–2758.

Harrington, R. F. 1961. *Time-Harmonic Electromagnetic Fields*. McGraw-Hill, New York.

Harrington, R. F. 1968. *Field Computation by Moments Methods*. IEEE Press, New York.

Haug, E. J., K. K. Choi, V. Komkov. 1986. *Design Sensitivity Analysis of Structural Systems*. Academic Press, Orlando, FL.

Jing, J. 2002. *The Finite Element Method in Electromagnetics*, 2nd ed. Wiley & Sons, New York.

Johns, D., C. Christopoulos. 1994. New frequency-domain TLM method for the numerical solution of steady-state electromagnetic problems. *IEE Proc. Sci. Measurement Tech.* **141** 310–316.

Lee, H. B., H. K. Jung, S. Y. Hahn. 1995. Shape optimization of H-plane waveguide tee junction using edge finite element method. *IEEE Trans. Magnetics* **31** 1928–1931.

Madsen, N. 1995. Divergence preserving discrete surface integral methods for Maxwell's equations using nonorthogonal unstructured grids. *J. Comput. Phys.* **119** 34–45.

Madsen, K., H. B. Nielsen, J. Søndergaard. 2002. Robust subroutines for non-linear optimization. Report IMM-REP-2002-02, Informatics and Mathematical Modeling, Technical University of Denmark, DK-2800 Kongens Lyngby, Denmark.

Nikolova, N. K., J. W. Bandler, M. H. Bakr. 2004. Adjoint techniques for sensitivity analysis in high-frequency structures CAD. *IEEE Trans. Microwave Theory Tech.* **52** 403–419.

Pasalic, D., R. Vahldiech, J. Hesselbarth. 1999. The frequency-domain TLM method with absorbing boundary conditions. *IEEE MTT-S Internat. Microwave Sympos. Digest*, 1669–1672.

Pozar, D. M. 1993. *Microwave Engineering*. Addison-Wesley Publishing Company, New York.

Sainati, R. A. 1996. *CAD of Microstrip Antennas for Wireless Applications*. Artech House, Boston, MA.

Webb, J. P. 2001. Design sensitivity using high-order tetrahedral vector elements. *IEEE Trans. Magnetics* **37** 3600–3603.

Webb, J. P. 2002. Design sensitivity of frequency response in 3-D finite-element analysis of microwave devices. *IEEE Trans. Magnetics* **35** 1109–1112.

Yee, K. S. 1966. Numerical solutions of initial boundary value problems involving Maxwell's equations in isotropic media. *IEEE Trans. Antennas Propagation* **14** 302–307.